

## Supporting Information

# Morphology and Element Doping Effect : Phosphorus-Doped Hollow Polygonal g- C<sub>3</sub>N<sub>4</sub> Rods for Visible Light-Driven CO<sub>2</sub> Reduction

Wen-Feng Wang<sup>a</sup>, Li-Qi Qiu<sup>b</sup>, Kai-Hong Chen<sup>b</sup>, Hong-Ru Li<sup>b</sup>, Lie-Feng Feng<sup>a\*</sup>,  
Liang-Nian He<sup>b\*</sup>

<sup>a</sup> *Tianjin Key Laboratory of Low Dimensional Materials Physics and Preparing  
Technology, Department of Applied Physics, School of Science, Tianjin University,  
Tianjin 300350, China*

<sup>b</sup> *State Key Laboratory and Institute of Elemento-Organic Chemistry, College of  
Chemistry, Nankai University, Tianjin 300071, China*

Corresponding author: Liefeng Feng; +86-18622730034; [fengliefeng@tju.edu.cn](mailto:fengliefeng@tju.edu.cn)

Corresponding author: Liang-Nian He; +86-22-23503878; [heln@nankai.edu.cn](mailto:heln@nankai.edu.cn)

### Quantitative analysis of product gases

After the reaction, partial gaseous products (1 mL) were taken from the tube using a syringe, and then analyzed by gas chromatography (GC, FuLi 9790II) with a TCD detector to determine the moles of CO. Afterwards, the total moles of CO obtained in the photocatalytic CO<sub>2</sub> reduction was calculated with the headspace volume of the Schlenk tube.

$$V_{co} = (S_{co}/S_{co(1mL)}) / \left( \frac{S_{H_2}}{S_{H_2(1mL)}} + \frac{S_{co_2}}{S_{Hco_2(1mL)}} + \frac{S_{co}}{S_{co(1mL)}} \right) \cdot V_{tube} \quad (1)$$

$$V_{H_2} = (S_{H_2}/S_{H_2(1mL)}) / \left( \frac{S_{H_2}}{S_{H_2(1mL)}} + \frac{S_{co_2}}{S_{Hco_2(1mL)}} + \frac{S_{co}}{S_{co(1mL)}} \right) \cdot V_{tube} \quad (2)$$

$$n_{co} = P \cdot V_{co} / RT \quad (3)$$

$$n_{H_2} = P \cdot V_{H_2} / RT \quad (4)$$

$$Selectivity(S) = \left[ \frac{n_{co}}{(n_{co} + n_{H_2})} \right] \cdot 100\% \quad (5)$$

where  $S_{H_2}$ ,  $S_{CO}$ ,  $S_{CO_2}$  represent the integral areas in the gas chromatography spectra (Shown as Fig. S3) of H<sub>2</sub>, CO and CO<sub>2</sub> for 1 mL gaseous products respectively.  $S_{H_2(1mL)}$ ,  $S_{CO(1mL)}$ ,  $S_{CO_2(1mL)}$  represent the integral areas for 1 mL pure H<sub>2</sub>, 1 mL pure CO and 1 mL pure CO<sub>2</sub>, respectively. In addition,  $V_{tube}$  (mL),  $V_{CO}$  (mL) and  $V_{H_2}$  (mL) is the headspace volume of the Schlenk tube and the volume of CO and H<sub>2</sub> in the total gaseous products. And  $n_{co}$  (μmol) and  $n_{H_2}$  (μmol) represent the total moles of CO and H<sub>2</sub> in the headspace of the Schlenk tube.

### Quantum efficiency calculation

Measurement of the Number of Moles of Photons: To a 25 mL flask, Ru(bpy)<sub>3</sub>Cl<sub>2</sub> (0.1 mM), 1,9-diphenylanthracene (DPA, 0.1 mM) and 25 mL acetonitrile were added. After that, the absorbance at 372 nm was recorded as  $A_{INITIAL}$ . Then, the sample was irradiated under 500 W Xenon long-arc lamp ( $\lambda \geq 400$  nm) for 10 min and a new UV-Vis spectra of sample at 372 nm was recorded, which was denoted as  $A_{FINAL}$ . The equation below was used to calculate the moles of consumed DPA.

$$\text{moles DPA consumed} = \left( \frac{A_{INITIAL} - A_{FINAL}}{\epsilon_{372nm} l} \right) \times V$$

Where  $A_{\text{INITIAL}}$  and  $A_{\text{FINAL}}$  are the absorbance of the solution at 372 nm before and after irradiation, respectively;  $\epsilon_{372\text{nm}}$  is the extinction coefficient of DPA at 372 nm in acetonitrile ( $11000 \text{ M}^{-1}\text{cm}^{-1}$ ),  $l$  is the path length of the cuvette (1 cm), and  $V$  is the volume of sample for which the absorption was measured (3 mL). Since the quantum yield ( $\Phi$ ) for  $\text{Ru}(\text{bpy})_3\text{Cl}_2$  is known to be 0.019, the moles of photons absorbed by our sample per unit time  $\frac{Nh\nu}{t}$  were determined using the consumed moles of DPA by following equation:

$$\frac{Nh\nu}{t} = \frac{\text{moles of DPA consumed}}{\Phi t}$$

Where  $\Phi$  is quantum yield of DPA consumption and  $t$  is the irradiation time (seconds).

To determine the  $\Phi_{\text{CO}}$  in our reaction, we applied the equation:

$$\Phi_{\text{CO}}(\%) = \frac{\frac{\# \text{ moles of CO}}{t'} \times 2}{\frac{Nh\nu}{t}} \times 100\%$$

Where  $t'$  is the reaction time for photocatalytic  $\text{CO}_2$  reduction and  $\frac{Nh\nu}{t}$  is the number of photons absorbed by the sample per unit time.

### Effect of P-doping level and morphology of g- $\text{C}_3\text{N}_4$ on the activity

In order to further confirm the effect of P doping and morphology change on the performance g- $\text{C}_3\text{N}_4$ , the P-doped g- $\text{C}_3\text{N}_4$  with different P contents were prepared in the same way as P-HCNR by changing the amount of phosphoric acid used in the preparation process. Specifically, 4 mL and 2 mL phosphoric acid were added to the melamine aqueous solution and the pH values of the resulting solutions were 2.5 and 3.5 respectively with vigorous stirring for 1 h. And then, the mixture was transferred into a 500 mL Teflon-lined stainless-steel autoclave for subsequent hydrothermal reaction at 180 °C for 6 h. The obtained mixture was filtered, washed with a small amount of deionized water and dried in an oven at 80 °C for 6 h. Finally, the obtained solid was calcined at 550 °C for 4 h in the tube furnace under argon atmosphere, affording the final product denoted as P-HCNR2 and P-HCNR3.

Moreover, the common P-doped g- $\text{C}_3\text{N}_4$  denoted as P-CN was also prepared. In detail, 3 g melamine and 6 mL phosphoric acid (85%) were dissolved in 300 mL deionized water and stirred for 1 h. Subsequently, the mixture was filtered and dried in

an oven at 80 °C for 6 h. Finally, the final P-CN was obtained by calcining at 550 °C for 4 h in the tube furnace under argon atmosphere.

Subsequently, the activities of photocatalytic CO<sub>2</sub> reduction were tested and compared. The activities of all samples were displayed in Table S2.

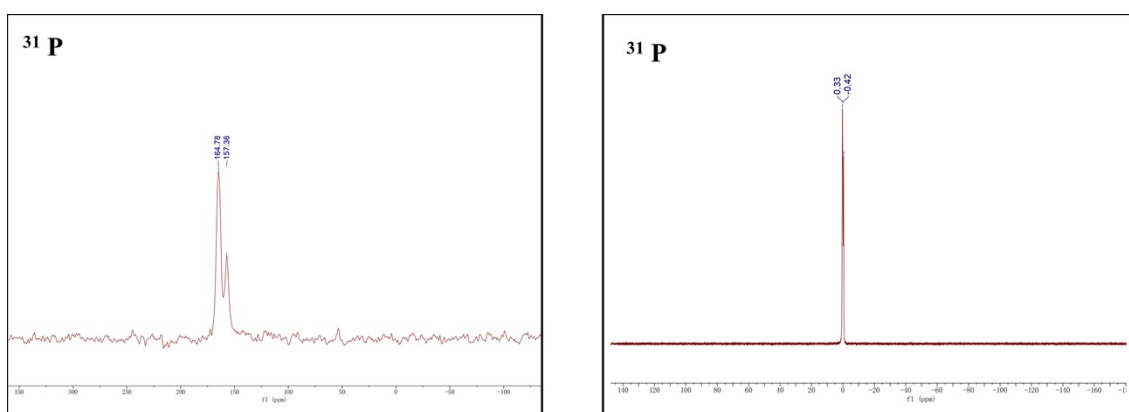


**Fig. S1.** <sup>31</sup>P MAS NMR spectra of P-HCNR and <sup>31</sup>P NMR of H<sub>3</sub>PO<sub>4</sub> (162 MHz, CDCl<sub>3</sub>).

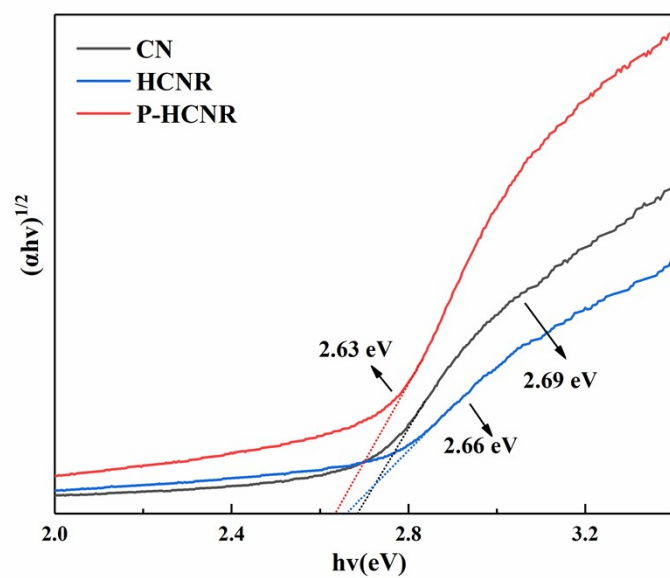


**Fig. S2.** Tauc plots of CN, HCNR and P-HCNR.



**Fig. S3.** Gas chromatography of product gases.

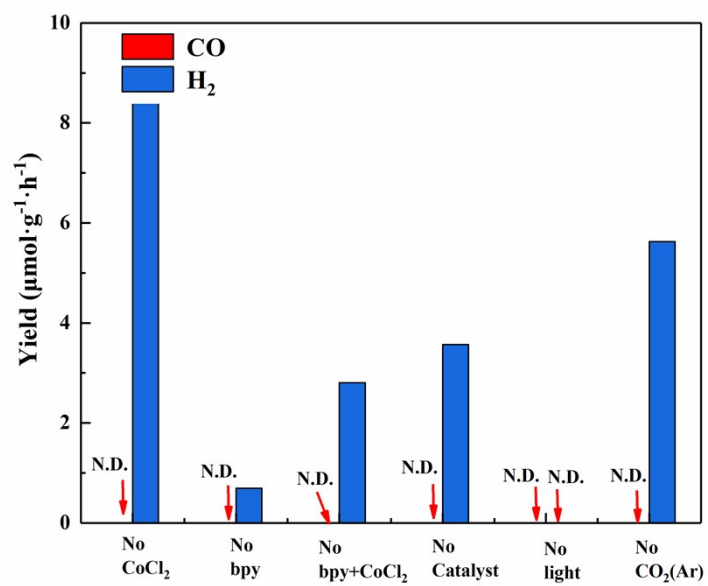


Figure. S4. Control experiments.

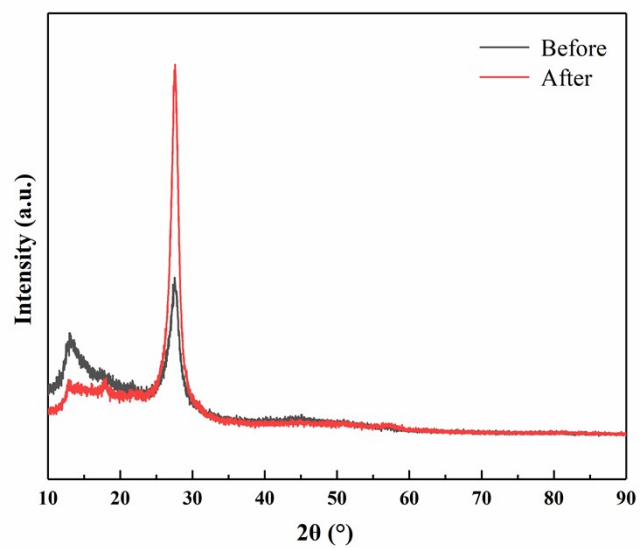


Figure. S5. XRD patterns of the P-HCNR before and after 10 hours' photocatalytic CO<sub>2</sub> reduction reaction.

**Table S1** Effect of CoCl<sub>2</sub> amount on CO/H<sub>2</sub> evolution and selectivity to CO.

Entry	CoCl <sub>2</sub> (μmol)	CO(μmol/g·h)	H <sub>2</sub> (μmol/g·h)	Selectivity (%)
1	0	0	8.43	/
2	0.1	81.29	1.65	98
3	0.5	227.41	4.89	98
4	1	447.53	16.05	97
5	1.5	280.10	6.68	97
6	2	227.42	4.89	97
7	4	78.86	3.23	96

**Table S2** CO/H<sub>2</sub> evolution and selectivity to CO for CN · HCNR, P-HCNR, P-HCNR2 and P-HCNR3.

Entry	Sample	CO(μmol/g·h)	H <sub>2</sub> (μmol/g·h)	Selectivity (%)
1	CN	67.01	3.55	94
2	HCNR	256.40	24.17	91
3	P-HCNR	447.53	16.05	96
4	P-CN	121.34	2.43	98
5	P-HCNR2	120.54	3.34	97
6	P-HCNR3	83.02	1.93	97

**Table S3** Control experiments.

Entry	Condition <sup>a</sup>	CO(μmol/g·h)	H <sub>2</sub> (μmol/g·h)
1	no CoCl <sub>2</sub>	0	8.44
2	no bpy	0	0.69
3	no bpy +CoCl <sub>2</sub>	0	2.80
4	no catalyst	0	3.56
5	dark	0	0
6	Ar	0	5.62

<sup>a</sup>Deviation from standard method

Materials	Cocatalyst	Products and Activity	Sacrificial agent	References
P-HCNR	[Co(bpy) <sub>3</sub> ]Cl <sub>2</sub>	CO: 447.5 mol/g·h Selectivity = 96%	TEOA	This work
C-doped BN nanosheet	[Co(bpy) <sub>3</sub> ]Cl <sub>2</sub>	CO: 93 μmol/g·h Selectivity = 76%	TEOA	[1]
mtw-CNT	[Co(bpy) <sub>3</sub> ]Cl <sub>2</sub>	CO: 253.3 μmol/g·h Selectivity = 96%	TEOA	[2]
Co <sup>2+</sup> doped 0D/2D TiO <sub>2</sub> /g-C <sub>3</sub> N <sub>4</sub>	[Co(bpy) <sub>3</sub> ]Cl <sub>2</sub>	CO: 290 μmol/g·h /	TEOA	[3]
TiO-CN	[Co(bpy) <sub>3</sub> ]Cl <sub>2</sub>	CO: 283.9 μmol/g·h Selectivity = 89%	TEOA	[4]
P-doped inverse opal g-C <sub>3</sub> N <sub>4</sub>	/	CO: 31.2 μmol/g·h Selectivity = 91%	H <sub>2</sub> O (gas)	[5]
Ultra-thin porous g-C <sub>3</sub> N <sub>4</sub> (THCN)	/	CO: ~1.8 μmol/g·h CH <sub>4</sub> : ~2.1 μmol/g·h	TEOA	[6]
Co <sub>1</sub> -C <sub>3</sub> N <sub>4</sub> /α-Fe <sub>2</sub> O <sub>3</sub>	/	CO: 14.9 μmol/g·h Selectivity > 99%	H <sub>2</sub> O (gas)	[7]
WO <sub>3</sub> /g-C <sub>3</sub> N <sub>4</sub>	/	CO: 41.47 μmol/g·h CH <sub>4</sub> : 0.75 μmol/g·h	TEOA	[8]

**Table S4** Comparison of photocatalytic CO<sub>2</sub> reduction performance with C<sub>3</sub>N<sub>4</sub> based materials.

#### Reference:

- [1] C. Huang, C. Chen, M. Zhang, L. Lin, X. Ye, S. Lin, M. Antonietti, X. Wang, Carbon-doped BN nanosheets for metal-free photoredox catalysis, *Nat. Commun.*, 2015, **6**, 7698.
- [2] Y. Chen, X. He, D. Guo, Y. Cai, J. Chen, Y. Zheng, B. Gao, B. Lin, *J. Energy Chem.*, 2020, **49**, 214–223.
- [3] H. Shi, J. Du, J. Ho, W. Ni, C. Song, K. Li, G. G. Gurzadyan, X. Guo, *J. CO<sub>2</sub> Util.*, 2020, **38**, 16–23.



- [4] S. Tang, X. Yin, G. Wang, X. Lu, and T. Lu, *Nano Res.*, 2019, **12**, 457–462.
- [5] X. Huang, W. Gu, S. Hu, Y. Hu, L. Zhou, J. Lei, L. Wang, Y. Liu and J. Zhang, *Catal. Sci. Technol.*, 2020, **10**, 3694–3700.
- [6] B. Yang, J. Zhao, W. Yang, X. Sun, R. Wang, X. Jia, *J. Colloid Interface Sci.*, 2021, **589**, 179–186.
- [7] B.-C. He, C. Zhang, P.-P. Luo, Y. Li, T.-B. Lu, *Green Chem.*, 2020, **22**, 7552–7559.
- [8] X. Li, X. Song, C. Ma, Y. Cheng, D. Shen, S. Zhang, W. Liu, P. Huo, and H. Wang, *ACS Appl. Nano Mater.* 2020, **3**, 1298–1306